



**HAL**  
open science

## Volume and surface area of Holstein dairy cows calculated from complete 3D shapes acquired using a high-precision scanning system: Interest for body weight estimation

Yannick Le Cozler, C. Allain, Caroline Xavier, L. Depuille, Anaïs Caillot, J.M. Delouard, L. Delattre, T. Luginbuhl, Philippe Faverdin

### ► To cite this version:

Yannick Le Cozler, C. Allain, Caroline Xavier, L. Depuille, Anaïs Caillot, et al.. Volume and surface area of Holstein dairy cows calculated from complete 3D shapes acquired using a high-precision scanning system: Interest for body weight estimation. *Computers and Electronics in Agriculture*, 2019, 165 (104977), pp.104977. 10.1016/j.compag.2019.104977. hal-02286677

**HAL Id: hal-02286677**

<https://institut-agro-rennes-angers.hal.science/hal-02286677>

Submitted on 23 Aug 2022

**HAL** is a multi-disciplinary open access archive for the deposit and dissemination of scientific research documents, whether they are published or not. The documents may come from teaching and research institutions in France or abroad, or from public or private research centers.

L'archive ouverte pluridisciplinaire **HAL**, est destinée au dépôt et à la diffusion de documents scientifiques de niveau recherche, publiés ou non, émanant des établissements d'enseignement et de recherche français ou étrangers, des laboratoires publics ou privés.



Distributed under a Creative Commons Attribution - NonCommercial 4.0 International License

1 **Volume and surface area of Holstein dairy cows calculated from complete 3D**  
2 **shapes acquired using a high-precision scanning system: interest for body**  
3 **weight estimation**

4  
5 *Y. Le Cozler<sup>(1)\*</sup>, C Allain<sup>(2)</sup>, C Xavier<sup>(1)</sup>, L. Depuille<sup>(2)</sup>, A. Caillot<sup>(1)</sup>, J.M. Delouard<sup>(3)</sup>, L.*  
6 *Delattre<sup>(3)</sup>, T. Luginbuhl<sup>(3)</sup>, P. Faverdin<sup>(1)</sup>*

7 (1) PEGASE, Agrocampus-Ouest, INRA, 35590 Saint-Gilles, France

8 (2) Institut de l'Élevage, Monvoisin, 35652 Le Rheu, France

9 (3) 3D Ouest, 5 Rue de Broglie, 22300 Lannion, France

10

11 \* Corresponding author: [yannick.lecozler@agrocampus-ouest.fr](mailto:yannick.lecozler@agrocampus-ouest.fr)

12

13 **Abstract**

14 Three-dimensional (3D) imaging is a solution for monitoring morphology and growth  
15 of dairy cows, but it can also estimate indicators such as body volume, surface area  
16 and body weight. A 3D full-body scanning device was used to scan 64 lactating  
17 Holstein cows from March-June 2018. The cows were individually and automatically  
18 weighed at a static weighing station (mean  $\pm$  standard deviation =  $673 \pm 65$  kg).  
19 These measured weights were compared to those predicted from regression models  
20 based on volume, area or morphological traits determined from 177 3D images.  
21 Since some images were truncated due to cow movement or technical problems, we  
22 developed additional regression models to reconstruct total volume or area. The  
23 accuracy of volume and area measurements was first tested on an inert cylindrical  
24 form (coefficients of variation (CVs)  $< 0.72\%$ ). The CVs for repeatability and  
25 reproducibility of the method of calculating volume and area from truncated images

26 were 0.17% and 3.12%, respectively. Cow volume and area ranged from 0.61-0.96  
27 m<sup>3</sup> and 5.80-8.32 m<sup>2</sup> respectively. Five regression models were developed to  
28 estimate cow body weight. Their coefficients of determination ranged from 0.82-0.93  
29 with prediction errors of ca. 3% (20 kg) and 4% (29 kg) as a function of volume and  
30 area, respectively. The device and the method, evaluated and validated in this study,  
31 offer the possibility to use new indicators such as body volume and area in precision  
32 livestock farming.

33

34 Keywords: volume, area, cows, sensors, 3D images, weight estimation

35

## 36 **1. Introduction**

37 New technologies based on image analysis are successfully used to improve  
38 management of most types of animal production. They have been developed to  
39 detect lameness in cows (van Hertem et al., 2014; Zhao et al., 2018) or to measure  
40 body parameters such as body condition score (BCS; Halachmi et al., 2008; Fischer  
41 et al., 2015; Sploliansky et al., 2016). Two-dimensional (2D) image approaches used  
42 in the past (Marchant et al., 1993; Schofield et al., 1998) were less effective due to  
43 the lack of a third dimension, distortion problems, the complexity of calibration and  
44 the need for multiple cameras and three-dimensional (3D) reconstruction models.  
45 Inexpensive 3D cameras (< 300 €) are now available, which increases the interest in  
46 3D approaches. They have been used to analyze BCS in dairy cattle, using either a  
47 fixed (Fischer et al., 2015) or mobile (Kuzuhara et al., 2015) device. Other authors  
48 (Negretti et al., 2008; Buranakarl et al., 2012; Guo et al., 2017; Pezzuolo et al., 2018)  
49 have also developed and used 3D imaging technologies for a wider variety of  
50 livestock. In most cases, animals were measured under laboratory conditions (heavy

51 equipment and landmarks on animals to guide computer measurements), which  
52 provided images of the entire body of restrained animals or portions of the body of  
53 unrestrained animals.

54 Equipment can often be adapted to farm conditions and recent literature describes  
55 devices used to estimate body weight (BW) of pigs in barns (Pezzuolo et al., 2018;  
56 Wang et al., 2018) and broilers in houses (Mortensen et al., 2016). Inexpensive and  
57 portable equipment based on the Microsoft Kinect® v1 sensor have often been used;  
58 however, authors concluded that most methods needed additional technical  
59 development to acquire and extract data automatically. Using 3D image technology to  
60 estimate animal BW is also of interest, since it reduces risky situations for both  
61 animals and humans and can provide frequent records. This technology is also  
62 suitable for collecting information about animal volume and area. For example, to  
63 examine heat stress in an increasingly warm environment, it would be useful to focus  
64 on area, since evaporative heat loss in most mammals occurs via perspiration from  
65 the skin and respiration (Berman, 2011).

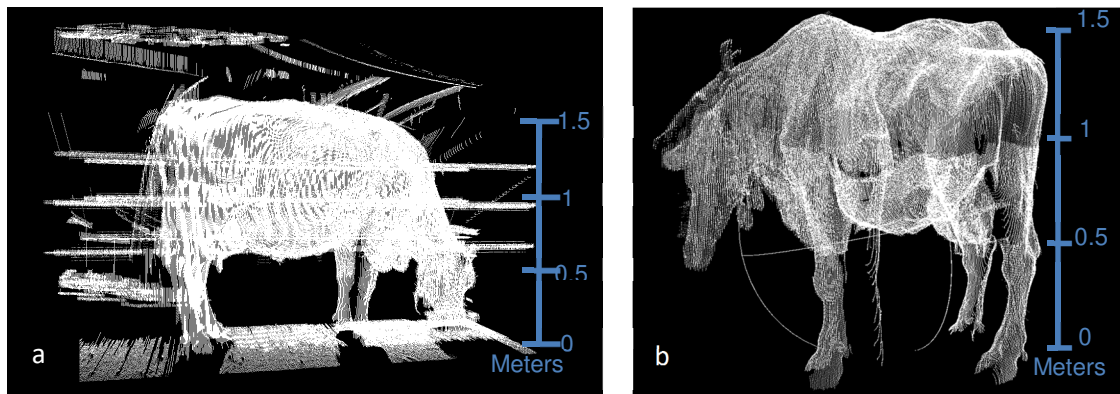
66 The Morpho3D scanning device was developed to record and monitor morphological  
67 traits (Le Cozler et al., 2019). In the present study, we tested the hypothesis that it  
68 could also determine volume and area of dairy cows accurately and thus their BW.

69

## 70 **2. Materials and methods**

71 **2.1. Animals:** Data were obtained from the INRA-UMR PEGASE experimental dairy  
72 station at Méjusseume, Le Rheu, in western France (48°11' N; 1°71' W; elevation 35  
73 m). The study involved 64 Holstein dairy cows with a mean BW of 673 kg (standard  
74 deviation (SD) = 65 kg) and parity ranging from 1-5. After each milking (twice a day),  
75 cows were individually and automatically weighed at a static weighing station

76 (DeLaval France, Elancourt, France) at the milking parlor's exit. Mean BCS, based on  
77 the French scoring scale of 0-5 (Bazin et al., 1984), was 2.05 ( $\pm$  0.25). One month,  
78 after weighing, cows were scanned with the Morpho3D device (section 2.3). Data  
79 were collected from March-June 2018, yielding 289 3D images. However, due to  
80 abnormal behavior of the cows or excessive light in May (which generated artifacts  
81 on images), cloud points were considered of too low quality to be used for 3D images  
82 reconstruction (Fig.1). As a result, only 177 3D images were used to estimate  
83 morphological traits, volume and area.



84 Figure 1. Examples of poor quality cloud points due to (a) excessive light or (b) animal  
85 movement.

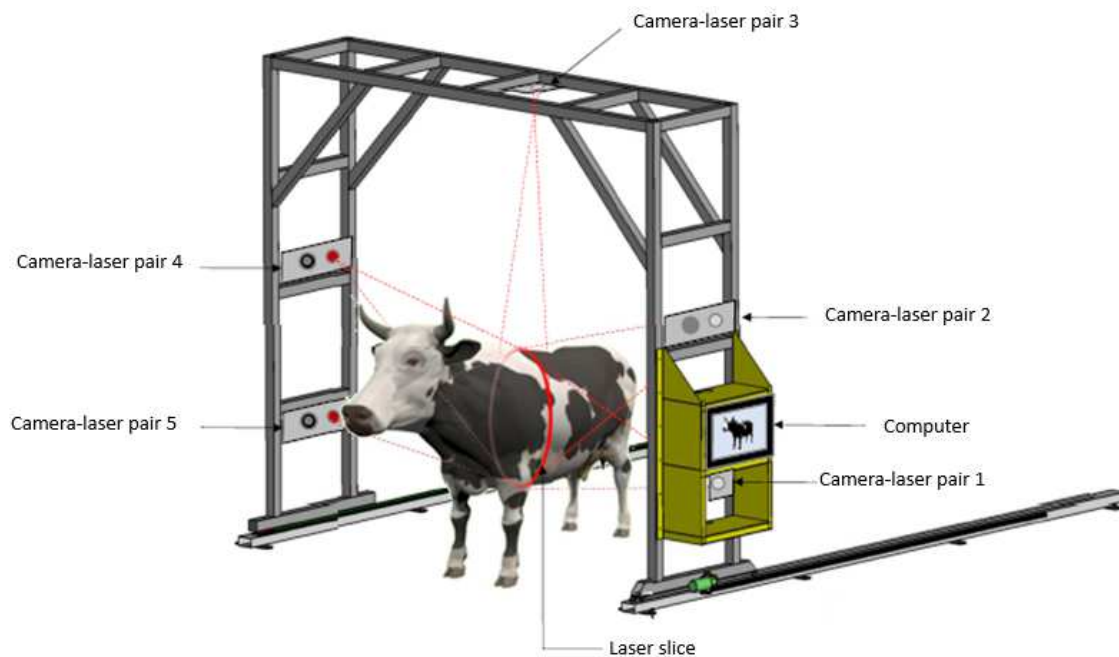
86

87 To limit image quality problems due to animal movements and excess light, the  
88 Morpho3D device was then partially covered with an opaque tarpaulin and the  
89 installation of a feed fence limited the cow movement.

90

91 **2.2. Cylinder model:** A cylinder model, on which measurements could be performed  
92 easily and precisely, was scanned to determine the accuracy of measurements and  
93 calculations of volumes and areas from 3D images. The cylinder model was  
94 considered the reference object, and its volume and area were measured manually  
95 and calculated.

96 **2.3. Morphological acquisition system:** 3D images of the cows were acquired  
97 automatically using Morpho3D, a sliding acquisition system, located near the  
98 weighing station (Fig. 2). Briefly, the system had five cameras, each paired with a  
99 laser projector. The VGA image resolution of each camera was  $640 \times 480$  pixels. Two  
100 cameras were fixed at 0.40 and 1.77 m above ground level, respectively, on each  
101 side of the portal. The fifth camera was fixed to the middle of the top of the portal  
102 (3.00 m above ground level). The portal moved at a mean speed of  $0.5 \text{ m}\cdot\text{s}^{-1}$  from  
103 back to front (phase 1) and returned to its initial position at a mean speed of  $0.3 \text{ m}\cdot\text{s}^{-1}$   
104 (phase 2). Each camera took 80 images per second only during phase 1, yielding a  
105 total of 2,000 images. The cameras were attached to the sliding portal ( $l = 5.00 \text{ m}$ ;  $w$   
106  $= 2.58 \text{ m}$ ;  $h = 3.00 \text{ m}$ ; Fig. 2). See Le Cozler et al. (2019) for additional details about  
107 Morpho3D.



108  
109 Figure 2. Design of the Morpho3D scanner

110  
111 Reconstructing an animal in 3D is a generalization of laser triangulation. Each  
112 Morpho3D laser generates a vertical plane, whose intersection with the object

113 appears as a stripe in each image, yielding more points per image. Knowing the  
114 equation of the plane in the camera frame allows the 3D position of the points in each  
115 stripe in the camera frame to be determined by intersecting the plane with the ray  
116 passing through the origin of the camera and the points observed in the image plane.  
117 Sliding the system's portal horizontally scans the laser plane over the entire object,  
118 yielding a point cloud consisting of several "slices" of 3D points (1 slice = 1 image).  
119 These point slices are aggregated based on the location of the system's portal. The  
120 cameras were calibrated using a black-and-white checkerboard placed in different  
121 locations in the Morpho3D device. Each camera-laser pair was calibrated individually  
122 and then two-by-two to calibrate all five cameras collectively. Images of the laser  
123 stripes projected onto the cow were captured by their corresponding camera and sent  
124 to a computer to reconstruct the cows' 3D information. First, images from each  
125 camera were processed to build separate point clouds using calibration information  
126 and the speed of the portal. A 3D reconstruction of the entire cow was generated by  
127 recording and merging the multiple 3D point clouds from the five camera-laser pairs.  
128 This resulted in a single point cloud representation of the entire cow.

129 Two camera filters were used during image capture: a physical filter centered on the  
130 laser wavelength to reduce ambient light and increase the contrast of laser stripes in  
131 each image and a software filter to prevent recording of undesirable points too far  
132 from the camera. Undesired objects were deleted during a cleaning process using  
133 Metrux2α® software (3D Ouest, Lannion, France). This step ensured that the point  
134 cloud is a sampling of a smooth surface on which surface normal vectors can be  
135 estimated. Finally, surface normals were estimated from the point cloud, and a  
136 screened Poisson surface-reconstruction algorithm was applied to build a  
137 triangulated mesh (Kazhdan and Hoppe, 2013) using Meshlab® open-source

138 software (Cignoni et al., 2008).

139

## 140 **2.4. Calculating volume and area**

### 141 **2.4.1. Principles of calculating volume and area**

142 Metrux2α® was used to perform linear measurements and estimate morphological  
143 traits, volume and area. Le Cozler et al. (2019) describe the linear measurements  
144 and their validation. Volume and area were automatically calculated by algorithms  
145 integrated into Metrux2α®, similar to the method used for morphological traits. Area  
146 was calculated from a triangular 3D mesh created from a list of interconnected 3D  
147 vertices. Each vertex shared by several triangles was then indexed to identify its  
148 position in relation to the other vertices to create a list of triplets of vertices that form  
149 the triangles. From this list, the area of each triangle was calculated. The total area of  
150 the cow equaled the sum of the areas of the triangles of the 3D mesh.

151 Volume was calculated using the method of Mirtich (1996), based on divergence  
152 theorem and Green's theorem. In it, volume equals the volumetric integral of the  
153 characteristic function of the object, but this integral cannot be calculated directly for  
154 a complex volume. Instead, faces and points, from which calculations can be made,  
155 must be introduced. The divergence theorem transforms an integral of the volume  
156 into an integral of the area, as follows

$$157 \quad \int_v \nabla \cdot F \, dV = \int_{\delta v} F \cdot \hat{n} \, dA$$

158 where  $v$  is the volume,  $\delta v$  is the surface around the volume,  $\nabla$  is the nabla operator  
159 which characterizes the divergence,  $F$  is the vector field of the volume and  $n$  is the  
160 normal to the surface oriented towards the outside.

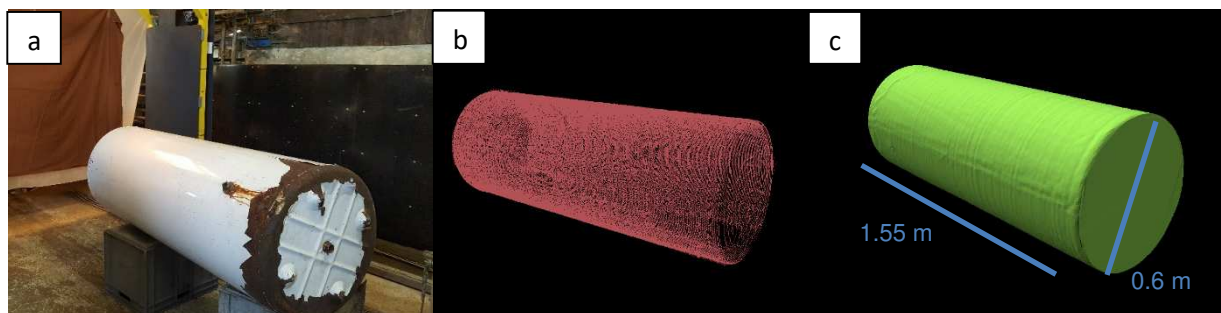
161 This divergence theorem is used on a vector field whose divergence is equal to 1 in  
162 order to find the characteristic function of the object. In a second step, the surface

163 around the volume is calculated using Green's theorem, which transforms the integral  
164 of the area of the triangles of the 3D mesh into an integral of the segments,  
165 themselves calculated from the 2D coordinates of the vertices. This step requires  
166 transforming the 3D coordinates into local 2D coordinates. The volume and area of  
167 the 3D image are then calculated from the vertices of the triangular 3D mesh.

168

#### 169 **2.4.2. Application to the cylinder model**

170 We first applied the method to calculate the volume and area of the cylinder model.  
171 After scanning, image acquisition and cleaning, a single point-cloud representation of  
172 the cylinder was obtained and a triangulated mesh was built (Fig. 3). This process  
173 was repeated 10 times to acquire 10 images. We then compared the volumes and  
174 areas calculated by Metrux2α® to those calculated by Meshlab®, since the latter is  
175 widely used for this purpose. We also compared the volume and area measured  
176 manually to those calculated by Metrux2α®.



177

178 Figure 3. Data acquisition from (a) the reference cylinder model (b) the raw point cloud after  
179 cleaning and (c) the final 3D image after Poisson surface-reconstruction.

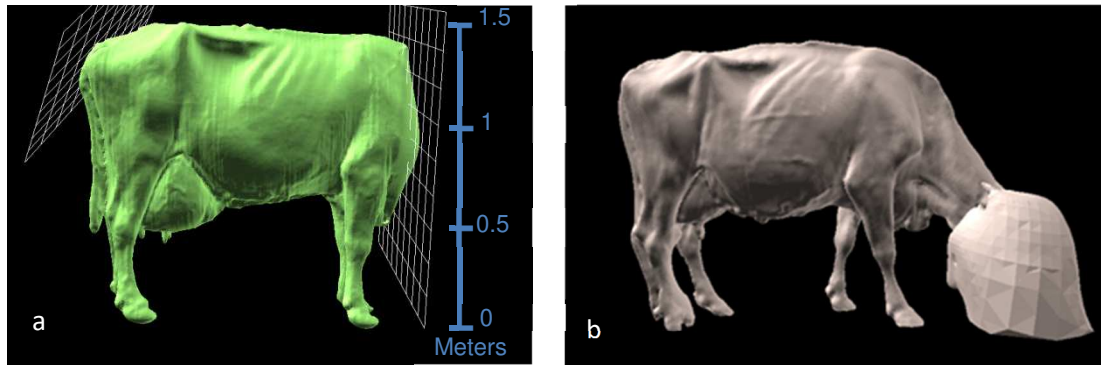
180

#### 181 **2.4.3. Application to living animals**

182 Due to animal movement, not all images could be used in full. Although the cow's  
183 body was digitized properly, its head usually moved, which sometimes distorted its

184 volume and area. It was sometimes necessary to restrain younger and/or nervous  
185 animals in a feed fence during image acquisition. As a result, the image was cut off at  
186 shoulder level (Fig. 4).

187



188 Figure 4. Images obtained when a cow was (a) restricted in a feeding fence (truncated  
189 image) or (b) its head moved too much during image acquisition.

190

191 To decrease cow movement without affecting the lasers, we provided concentrate  
192 feed in a rectangular bowl, either opaque plastic or transparent glass. The presence  
193 of the opaque plastic bowl changed the shape of the cow's volume (Fig. 5). The  
194 depth of the cow's head in the bowl at the time of acquisition varied, but the addition  
195 of the bowl to the cow's head added a maximum volume of 5 dm<sup>3</sup> and area of ca. 0.2  
196 m<sup>2</sup> (Fig. 5a). In some images, the bowl truncated the head, removing a mean volume  
197 of 3 dm<sup>3</sup> and a mean area of 0.1 m<sup>2</sup> (Fig. 5b). To avoid this bias, the transparent  
198 glass bowl was used, which did not distort the cow's head, allowing volume and area  
199 of the cow to be calculated accurately (Fig. 5c).

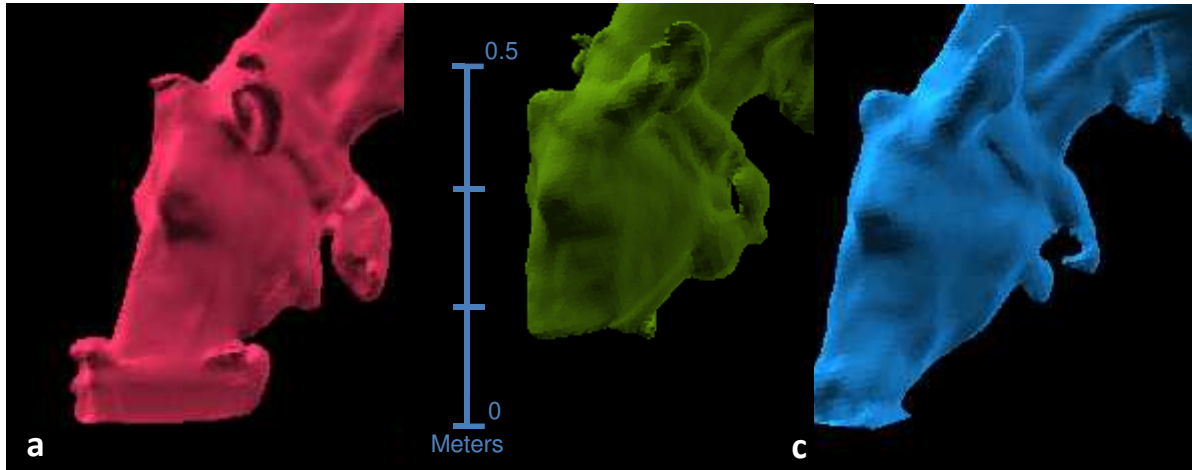
200

201

202

203

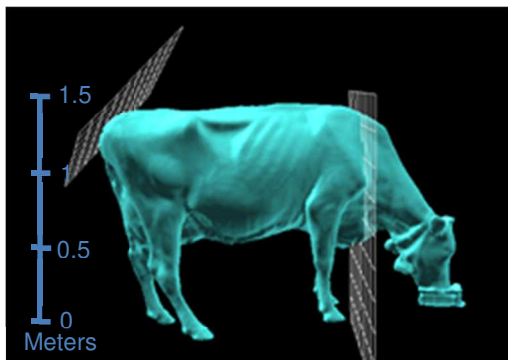
204  
205  
206  
207  
208  
209  
210



211 Figure 5. Differences in cow head reconstruction with (a) an opaque plastic bowl, (b) an  
212 opaque plastic bowl that truncates the head or (c) a transparent glass bowl.

213

214 Given the need to restrain some cows, we assessed the ability to estimate total  
215 volume and area from images of animals cut off at shoulder level. Only high-quality  
216 images (i.e. with the head scanned correctly) were selected. Two volumes and areas  
217 were determined on from the images: total volume and area, calculated using the  
218 automatic algorithm, and truncated volume and area, measured by placing one plane  
219 at the tip of the shoulder blades (similar to that used by Minagawa (1994)) and  
220 another at the rump (Fig. 6).



221

222 Figure 6. Position of the cutting planes used to estimate truncated volume and area when the  
223 head was missing from an image (i.e. cow restrained by a feed fence)

224

225 The two planes were placed using 3D image-processing software Metrux2α® after  
226 placing three points on the image (Fig. 5). The Metrux2α® was used to estimate the  
227 volume and area between the two planes and to measure six morphological traits  
228 from the images: heart girth, chest depth, wither height, hip width, backside width and  
229 ischial width. Details of these traits are available in Le Cozler et al. (2019).

230 Area and volume could be influenced by surface noise and some apparent  
231 roughness. Cleaning the resulting points cloud before creating the image required  
232 then patience and precision. Nevertheless, for some images, the reconstruction was  
233 sometimes not totally satisfactory (e. g. tail stuck to the animal, which was not the  
234 case on points cloud). But these errors were finally negligible, since the validation  
235 tests, carried out on different images of the same animals showed extremely small  
236 variations (see section 3.3).”

237

## 238 **2.5. Repeatability and reproducibility analyses**

239 As done for morphological traits (Le Cozler et al., 2019), we used the Morpho3D  
240 device to estimate the repeatability and reproducibility of calculating volume and  
241 area.

242

### 243 **2.5.1. Repeatability and reproducibility of plane placement**

244 Since total volume and area were calculated automatically, their repeatability and  
245 reproducibility did not require assessment (i.e. no variation among measurements  
246 due to the operator). For truncated images, however, the repeatability of plane  
247 placement and point identification was analyzed to determine whether, for a given  
248 image, the placement of planes was reliable and whether the same volume or area  
249 could be calculated. Five images of complete cows were used, on which the same

250 operator placed the cutting planes five times. Truncated volume and area were thus  
251 calculated five times from each of five different images.

252 For reproducibility, we assessed the ability of different operators to identify visually  
253 where to place the cutting planes. On images of five cows scanned only once, two  
254 operators repeated the placements five times each. In total, we assessed 50  
255 measurements (25 per operator) on five different images. Truncated volume and area  
256 were then calculated.

257

### 258 **2.5.2. Reproducibility of volume and area of the Mopho3D device in a changing** 259 **environment**

260 Analysis of reproducibility aimed to verify whether the method was able to calculate  
261 the same values from different image acquisitions in a changing environment caused  
262 by variability in cow position, image reconstruction and operator plane placements.  
263 Reproducibility was assessed using images of nine cows, each undergoing the entire  
264 procedure, from initial acquisition to calculation of volume and area, five times. The  
265 same operator performed all of the manipulations. In this procedure, the  
266 reproducibility combined the repeatability error of volume and area calculation with  
267 that of plane placement.

268

### 269 **2.5.3. Calculation**

270 Variability in volume and area calculated from the 3D images was corrected for the  
271 effect of individual cows by extracting residuals from an analysis of variance  
272 (ANOVA) model. Repeatability and reproducibility were estimated using the SDs of  
273 placement repeatability ( $\sigma_{rp}$ ), inter-operator reproducibility ( $\sigma_{Ro}$ ) and reproducibility in  
274 a changing environment ( $\sigma_{Ri}$ ). Values of  $\sigma_{rp}$  and  $\sigma_{Ri}$  were calculated from the residues

275 of the single-factor ANOVA of the individual-cow effect, while  $\sigma_{R_0}$  was calculated from  
276 the mean of the reproducibility SDs of an ANOVA of the operator effect. Existing  
277 variations among cows were then excluded from the analysis. The coefficients of  
278 variation of repeatability ( $CV_{rp}$ ) and those of inter-operator and changing environment  
279 reproducibility ( $CV_{R_0}$  and  $CV_{R_i}$ , respectively) were then estimated from their  
280 respective means ( $\mu_{rp}$ ,  $\mu_{R_0}$  and  $\mu_{R_i}$ , respectively) and SDs ( $\sigma_{rp}$ ,  $\sigma_{R_0}$  and  $\sigma_{R_i}$ ,  
281 respectively). The more repeatable (or reproducible) the 3D measurement, the  
282 smaller was its  $CV_{rp}$  (or  $CV_{R_0}$  or  $CV_{R_i}$ ).

283

## 284 **2.6. Estimation of body weight**

285 Cow BW was measured twice a day. BW was also predicted using several regression  
286 models based on morphological traits, volume and area calculated with the  
287 Morpho3D device. Predictions of these models were then compared to the BW  
288 measured with the weighing system. From the measurements performed on  
289 complete images, a correlation matrix of Pearson coefficients was calculated to  
290 identify relationships between traits. Volume, area and morphological traits were  
291 measured or/ calculated from 3D images, while other traits, such as BCS and BW,  
292 were available in the database of the herd management system.

293 Several linear regression models to predict BW from traits measured or calculated  
294 from the 3D images were tested. The models were developed using the Akaike  
295 information criterion (AIC) with "backward elimination" variable selection. This  
296 method begins with all variables and then removes one or more variables at each  
297 iteration until it obtains the minimum value of the AIC, defined as  $2 \times (n-2) \times \log(L)$ ,  
298 where  $n$  is the number of variables in the model and  $L$  is the maximum probability of  
299 the likelihood function. Each final model was cross-validated to estimate its prediction

300 error. Cross-validation was preferred due to the small size of the dataset, which  
301 precluded separating it into sufficiently large calibration and validation datasets. The  
302 dataset was thus randomly divided into 2 groups, one of them containing 90%of  
303 datasets. This large group was used to develop BW models, which were then  
304 validated on data from the remaining group. Ten iterations of each model were cross-  
305 validated 100 times using different random draws to obtain a large number of  
306 variations and calculate the root mean square error of prediction (RMSEP).  
307 Coefficient of determination ( $R^2$ ) and RMSEP of the models were calculated to  
308 determine the quality of the linear regression and quantify the mean prediction error  
309 made by the model during cross-validation, respectively.

310

## 311 **2.7. From truncated to complete images**

312 Total volume and area were predicted using regression models based on truncated  
313 images. As before, models were developed using AIC with "backward elimination"  
314 variable selection. The same variables, except for total volume and area, were used  
315 in the models. Two models for each variable (total volume and total area) were  
316 developed: one with multiple variables that minimized RMSEP and another with only  
317 truncated area or volume. As before, 10 iterations of each model were cross-  
318 validated 100 times using different random draws to obtain a large number of  
319 variations and calculate RMSEP.

320

## 321 **2.8. Statistical analysis**

322 All statistical analyses (i.e. ANOVA, repeatability, reproducibility, correlation analysis)  
323 were performed using R software (R Core Team, 2016).

324

325 **3. Results**

326 **3.1. Volume and area of the cylinder model**

327 The error in determining both volume and area of the cylinder model was 0.0005%  
328 for Metrux2α® and 0.0001% for Meshlab®. Differences between Metrux2α®  
329 estimates and manual measurements were less than 1%, regardless of the trait  
330 (Table 1).

331

332 Table 1. Mean and standard deviations (SD) of traits of the cylinder model estimated by the  
333 Morpho3D device (10 images) and absolute and relative differences between them and  
334 manual measurements.

Trait	Mean	SD	Difference	
			Absolute	Relative
Length (h), m	1.552	0.010	-0.010	0.62%
Circumference (d x π), m	1.880	0.005	-0.008	0.24%
Surface area (π x d x (h + d/2)), m <sup>2</sup>	3.490	0.015	-0.028	0.44%
Volume (π x (d/2) <sup>2</sup> x h), m <sup>3</sup>	0.440	0.003	-0.003	0.72%

335

336 **3.2. Volume and area of cows**

337 Morphological traits, volume and area were measured or calculated for the 64  
338 Holstein dairy cows (Table 2). Mean (± 1 SD) volume and area of cows was 0.76 (±  
339 0.07) m<sup>3</sup> and 6.84 (± 0.45) m<sup>2</sup>, respectively. Truncated volume and area equaled 90%  
340 and 81% of total volume and area, respectively. Density of the cows (i.e. BW/total  
341 volume) was 0.89 kg dm<sup>-3</sup>, but ranged 0.79 to 0.95 kg dm<sup>-3</sup>.

342

343

344 Table 2. Mean, standard deviation (SD), and minimum and maximum values of body weight,  
 345 body condition score (French scale of 0-5 (Bazin et al., 1984)), morphology, volume and area  
 346 of 64 dairy Holstein cows measured or calculated from 177 images. Truncated volume and  
 347 area were calculated from the tip of the shoulder blades to the rump by placing one plane at  
 348 each location.

Body trait	Mean	SD	Min.	Max.
Body weight, kg	673	65	539	871
<b>Body condition score</b>	<b>2.05</b>	<b>0.25</b>	<b>1.50</b>	<b>2.88</b>
Heart girth, cm	228	10	210	256
Chest depth, cm	85.9	3.2	78.8	95.3
Wither height, cm	146	5	135	160
Hip width, cm	58.8	3.4	50.7	66.7
Backside width, cm	53.8	2.7	44.3	63.5
Total volume, m <sup>3</sup>	0.76	0.07	0.61	0.96
Truncated volume, m <sup>3</sup>	0.69	0.07	0.56	0.84
Total area, m <sup>2</sup>	6.84	0.45	5.80	8.32
Truncated area, m <sup>2</sup>	5.53	0.39	4.60	7.17
<b>Density, kg dm<sup>-3</sup></b>	<b>0.89</b>	<b>0.03</b>	<b>0.79</b>	<b>0.95</b>

349

### 350 **3.3. Reproducibility and repeatability**

351 Repeatability estimated the error related to an operator's placement of planes on  
 352 truncated images. Placement of the planes varied little ( $\sigma_{rp}$  for volume and area =  
 353 0.17% and 0.32%, respectively). Inter-operator reproducibility had larger error,  $\sigma_{Ro}$  for  
 354 volume and area 1.00% and 1.80%, respectively. Reproducibility of total and

355 truncated values in a changing environment ( $\sigma_{Ri}$ ) had even higher errors (CVs for  
 356 both = ca. 2-3%) (Table 3). In calculations of total volume and area, CVs expressed  
 357 measurement error related to image acquisition and processing. In calculations of  
 358 truncated volume and area, CVs combined image acquisition and processing error  
 359 with plane-placement error.

360  
 361 Table 3. Reproducibility of total and truncated volume and area in a changing environment  
 362 assessed by standard deviation (SD) and coefficient of variation (CV). Truncated volume and  
 363 area were calculated from the tip of the shoulder blades to the rump by placing one plane at  
 364 each location.

Repeatability	Mean	SD	CV
Total volume, m <sup>3</sup>	0.78	0.02	2.24%
Truncated volume, m <sup>3</sup>	0.72	0.02	2.43%
Total area, m <sup>2</sup>	6.94	0.02	2.85%
Truncated area, m <sup>2</sup>	5.59	0.1	3.12%

365  
 366 **3.4. Estimating body weight from 3D images**  
 367 Traits measured from 3D images were strongly correlated with each other and with  
 368 BW (Table 4). BCS was not correlated with other variables (maximum  $r = 0.22$ ). BW  
 369 and volume (total or truncated) were strongly correlated ( $r = 0.93$  and  $0.92$ ,  
 370 respectively). Volume and area (total or truncated) were also strongly correlated ( $r =$   
 371  $0.84-0.87$ ).

372 Table 4. Correlation matrix between traits measured and/or estimated from 3D images. Truncated volume and area were calculated from the tip  
 373 of the shoulder blades to the rump by placing one plane at each location. (Under the diagonal: Pearson correlation coefficient; Above the  
 374 diagonal: p-value of the correlation). BCS: body condition score, BW: body weight.

Trait	Total volume	Truncated volume	Total area	Truncated area	Hip width	Wither height	Chest depth	Heart girth	Backside width	BCS	BW
<b>Total volume</b>	-	<0.001	<0.001	<0.001	<0.001	0.012	0.296	0.502	0.008	0.020	<0.001
<b>Truncated volume</b>	0.99	-	<0.001	<0.001	<0.001	0.012	0.298	0.535	0.008	0.018	<0.001
<b>Total area</b>	0.87	0.86	-	<0.001	0.004	0.017	0.407	0.948	0.025	0.007	0.003
<b>Truncated area</b>	0.84	0.86	0.94	-	0.005	0.019	0.485	0.871	0.027	0.010	0.004
<b>Hip width</b>	0.76	0.76	0.64	0.62	-	0.010	0.221	0.537	0.002	0.002	<0.001
<b>Wither height</b>	0.66	0.66	0.62	0.61	0.61	-	0.008	0.435	0.191	0.020	0.007
<b>Chest depth</b>	0.56	0.56	0.50	0.45	0.52	0.67	-	0.083	0.934	0.318	0.152
<b>Heart girth</b>	0.54	0.53	0.40	0.31	0.44	0.43	0.56	-	0.824	0.718	0.334
<b>Backside width</b>	0.61	0.61	0.53	0.50	0.61	0.38	0.30	0.26	-	0.001	0.004
<b>BCS</b>	0.15	0.14	0.04	0.01	-0.03	0.05	0.20	0.22	-0.12	-	0.031
<b>BW</b>	0.93	0.92	0.72	0.71	0.80	0.70	0.63	0.57	0.66	0.19	-

375

376 Since correlations between BW and the main traits were linear, linear regression  
 377 models (1) and (2) were developed with the maximum number of variables from  
 378 complete images using AIC (Table 5). After testing these more complex models, we  
 379 included only 1-3 variables in models (3) and (4).

380

381 Table 5. Models predicting body weight (BW, in kg) of cows as a function of selected traits  
 382 measured from complete images from the Morpho3D device. Model quality was assessed  
 383 with a coefficient of determination ( $R^2$ ) and root mean square error of prediction (RMSEP).

Model		BW		
		$R^2$	RMSEP	
(1)	$BW = 812.1 \times total\ volume - 81.4 \times area + 343.8 \times backside\ width + 273.8 \times hip\ width + 208.8 \times heart\ girth + 113.7 \times wither\ height - 280.7$	0.93	18.2	2.72%
(2)	$BW = 31.7 \times area + 608.8 \times hip\ width + 593.4 \times backside\ width + 257.2 \times wither\ height + 152.8 \times heart\ girth - 905.3$	0.82	29.3	4.38%
(3)	$BW = 620 \times total\ volume + 379 \times backside\ width + 287.7 \times hip\ width - 174$	0.88	22.5	3.36%
(4)	$BW = 827.5 \times total\ volume + 45.8$	0.85	24.9	3.72%
(5)	$BW = 102.3 \times total\ area - 30.33$	0.49	45.2	8.75%

384 For the selected traits, see corresponding units in tables 3 and 4

385 Model (1) was the most accurate (RMSEP = 2.72%,  $R^2 = 0.93$ ); it included six of nine  
 386 possible traits (BCS not included because of the lack of correlation) previously  
 387 mentioned): total volume, total area, hip width, backside width, wither height and  
 388 chest depth. However, the coefficient of collinearity between total volume and total  
 389 area was greater than 4 (not presented). Other models, free of strong collinearity and  
 390 therefore more generalizable, were tested, such as including area but not volume  
 391 (model (2)), or volume but not area (model (3)), but they were less accurate (RMSEP  
 392 = 3.36% and 4.70%, respectively). A 4<sup>th</sup> model, which considered only volume, was  
 393 only moderately accurate ( $R^2 = 0.85$ , RMSEP = 3.72%), which corresponded to an

394 error of 25 kg in predicted BW. In a similar way, a final model (5), which considered  
 395 only area, indicated a poor accuracy ( $R^2 = 0.49$ , RMSEP = 6.75%), which  
 396 corresponded to an error of 45 kg in predicted BW.

397

### 398 **3.5. Predicting total volume and area from truncated images**

399 Since it was not always possible to acquire complete images, total cow volume and  
 400 area were predicted from truncated images (Table 6). A model using only truncated  
 401 volume (model (5b) predicted total volume accurately ( $R^2=0.98$ , RMSEP = 1.05%),  
 402 and adding heart girth increased its accuracy (model (5a),  $R^2 = 0.99$ , RMSEP =  
 403 1.02%). A model using only truncated area predicted total area accurately (model  
 404 (6b),  $R^2 = 0.85$ , RMSEP = 2.22%), and adding heart girth and backside width  
 405 increased its accuracy (model (6a),  $R^2 = 0.90$ , RMSEP = 2.14%); however, it was still  
 406 less accurate than the prediction of total volume.

407

408 Table 6. Models estimating total volume or total area of cows from truncated images. Model  
 409 quality was assessed with a coefficient of determination ( $R^2$ ) and root mean square error of  
 410 prediction (RMSEP). Truncated volume and area were calculated from the tip of the shoulder  
 411 blades to the rump by placing one plane at each location.

Model		$R^2$	RMSEP	
(5a)	$Total\ volume = 1.0595 \times truncated\ volume + 0.0165 \times heart\ girth - 0.0149$	0.99	0.008	1.02%
(5b)	$Total\ volume = 1.0704 \times volume + 0.0154$	0.98	0.008	1.05%
(6a)	$Total\ area = 0.990 \times truncated\ area + 1.039 \times backside\ width + 0.518 \times heart\ girth - 0.365$	0.90	0.146	2.14%
(6b)	$Total\ area = 1.07 \times truncated\ area + 0.94$	0.85	0.152	2.22%

412 *For the selected traits, see corresponding units in tables 3 and 4*

413

#### 414 **4. Discussion**

415 Scanning an inert cylinder showed that the scanner could accurately acquire and  
416 calculate volume, area, length and circumference with less than 1% error. The  
417 validation process assessed image acquisition and processing and thus validated the  
418 overall accuracy of the method. This method can calculate volume and area with high  
419 reproducibility (CV = 2.24% and 2.43%, respectively). On living animals, the  
420 reproducibility coefficients for calculating volume and area were slightly higher due to  
421 manual manipulation (placement of planes) and were quantified by the repeatability  
422 of the placement of planes (0.17% and 0.32% for volume and area, respectively). A  
423 future study could calculate the repeatability and reproducibility of each step of the  
424 method to identify when the method becomes less accurate.

425

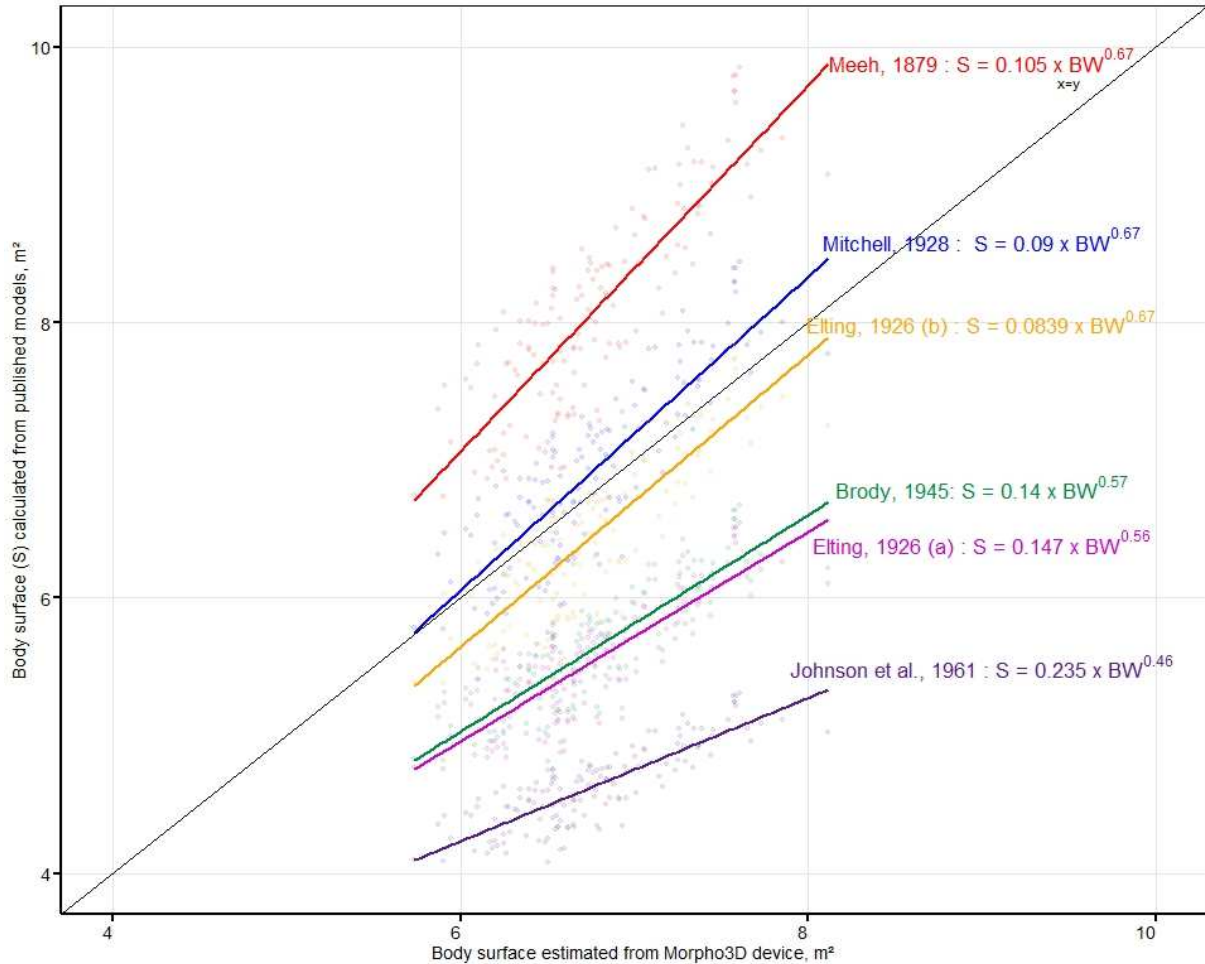
426 To assess the interest of developing this tool to render measurements automatic or  
427 semi-automatic, inter-operator reproducibility of plane placement was considered  
428 high (CVs for volume and area measurement = 1.00% and 1.80%, respectively).  
429 According to Fischer et al. (2015), a method is repeatable and reproducible when its  
430 CV is less than 3-5%. Unfortunately, repeatability and reproducibility tests are not  
431 widely available in the literature, even though they are essential for determining the  
432 relevance of tools and methods (Marinello et al., 2015). It is therefore difficult to  
433 compare the method we developed to other tools.

434

435 The model used most often to estimate body area was developed by Mitchell (1928):  
436  $0.14 \times BW^{0.67}$ . Other models are also available ((Elting 1926): (a):  $0.147 \times BW^{0.56}$ ,  
437 (b):  $0.0839 \times BW^{0.67}$ ; Brody (1945):  $0.14 \times BW^{0.57}$ ; Johnson et al., (1961):  $0.235 \times$   
438  $BW^{0.46}$ ). When we applied these models to the recorded BW in our database, some

439 yielded lower BW (Elting, 1926, model a; Brody, 1945; Johnson et al., 1961), similar  
440 BW (Elting et al., 1926, model b; Mitchell, 1928) or higher BW (Meeh, 1879) (Fig. 6).

441  
442



443  
444 Figure 6. Surface area of cows predicted by published models vs. those calculated using the  
445 Morpho3D device.

446  
447 Errors resulting from the image-reconstruction process or low-quality images may  
448 occur with the Morpho3D device. Other methods that estimate area, however, also  
449 have limits and can be difficult to use (e.g. the model of Mitchell (1928)). Future  
450 studies that accurately estimate area are needed with other methods than with  
451 Morpho3D device, but access to a large number of animals could be challenging, as  
452 well as determining area with such methods

453

454 Like for body area, little information is available on cow volume. Minagawa (1994)  
455 estimated the volume of the neck and head of beef cows, and the results indicated  
456 that the rest of the body's volume was similar to our truncated volume. By applying  
457 our model (5b, Table 6) to this truncated volume, we predicted less than 1.5%  
458 difference in the total volume for four of Minagawa's five cows. The difference in total  
459 area was less than 6%.

460

461 Validating the methods used to estimate morphological traits, volume and area from  
462 3D images enabled us to use these data to estimate cow BW, which is useful in  
463 breeding and feeding programs, commercial transactions and in the search for new  
464 indicators to estimate food-use efficiency in dairy animals. Estimation of BW,  
465 particularly during the rearing period, has been based for decades on development  
466 indicators (Heinrichs et al., 1992). It is indeed traditionally and commonly used in  
467 livestock production to follow growth of animals and/or then, adapt their feeding  
468 regimes. It is also used for commercialisation purposes for examples. Most feeding  
469 regimes for ruminants, pigs or poultry are based on animal body weight, which is  
470 rarely measured on-farms. As a result, recommendations are often based on visual  
471 estimation of BW. In addition, when performed so far, BW measurements are done  
472 manually, using weighing systems, which are also time consuming, sometimes costly,  
473 risky for human and animals health. Methods to estimate BW based on image  
474 technologies are then of increasing interest for many research groups, breeding  
475 organization, farmers and advisors. Estimating animal BW from measurements made  
476 from 3D images is a recent possibility (Anglart, 2010; Buranakarl et al., 2012;  
477 Kuzuhara et al., 2015). Anglart (2010) applied this approach to 3D acquisition of the

478 backs of Holstein dairy cows using a time-of-flight camera, obtaining a  $R^2$  for BW of  
479 0.87. Of the 6224 acquisitions, however, 30% of the BW estimated from the images  
480 had an error of more than 30 kg. Buranakarl et al. (2012) acquired full-body 3D  
481 images of buffaloes and developed 12 BW prediction equations (four each for all  
482 buffaloes, females and males) by changing the number of parameters considered.  
483 For females, they obtained an  $R^2$  for BW of 0.89 using four parameters (wither height,  
484 shoulder width, ischial width, length from ischia to shoulders). Kuzuhara et al. (2015)  
485 predicted BW from seven traits (RMSEP = 42 kg). The models used in the present  
486 study were therefore satisfactory ( $R^2 = 0.82-0.93$ , RMSEP from 2.72% (18.2 kg) to  
487 4.38% (29.3 kg)) compared to those previously published. Since only 16% of the BW  
488 had an error greater than 30 kg (model (3)), the scanner and the method used  
489 appear reliable. Unlike previous studies that used only linear traits as parameters, 3D  
490 imaging can create new models using volume and area. Ultimately, 3D imaging  
491 enables accurate and simplified estimation of BW from the traits measured,  
492 especially because it allows calculation of volume, which is strongly correlated with  
493 BW. Nevertheless, more automation (e.g. image preparation and measurement) is  
494 required to fully benefit from this tool.

495

## 496 **Conclusion and future studies**

497 The scanning technology described in this study provides new perspectives for  
498 assessing animal morphology and can be used to calculate volume and area of dairy  
499 cows. Analyses indicated that it was possible to estimate total volume and area from  
500 truncated images; however, all images had the same degree of truncation. Future  
501 studies are needed to determine whether other cutting planes (i.e. types of other  
502 types of truncation) could be useful. This suggests that truncated images from a less

503 complicated or portable device could be used in the future. In addition, the device  
504 can also be used to estimate BW which is useful information, without investing in a  
505 weighing system. Preliminary results also indicated that the device can estimate  
506 changes in volume in the short term (rumen content), medium term (embryo  
507 development) and long term (growth).

508 The Morpho3D device allowed the acquisition of new phenotypes, not accessible  
509 until now, such as area and volume, at high-flow rates. There were no plans to  
510 implement this device on a large scale in commercial farms. For this purpose, a new  
511 version, not depending on animal movements and not sensitive to ambient light, is  
512 being tested. The quality of the 3D-images is lower, but sufficient to estimate most  
513 parameters previously presented, that will be compared to values obtained from  
514 Morpho3D device, considered as "Gold Standards".

515

## 516 **Acknowledgments**

517 The authors wish to thank everyone involved in the Morpho3D project, especially  
518 technicians at the Méjusseume experimental station, who took excellent care of the  
519 animals. The Morpho3D project is supported by the National Fund CASDAR, which  
520 supports innovation in agriculture (RFP "Recherche Technologique" 2015, no. 005),  
521 special funds from the INRA Animal Physiology and Livestock Systems division for  
522 innovative projects and the collaborative ANR – APIS-GENE project DEFFILAIT.

523

## 524 **References**

525 Anglart, D., 2010. Automatic estimation of body weight and body condition score in dairy cows using  
526 3D imaging technique. Swedish University of Agricultural Sciences, Master's thesis.

527 Bazin, S., Augéard, P., Carteau, M., Champion, H., Chilliard, Y., Cuyllé, G., Disenhaus, C., Durand, G.,  
528 Espinasse, R., Gascoin, A., Godineau, M., Jouanne, D., Ollivier, O., Remond, B., 1984. Grille de

529 notation de l'état d'engraissement des vaches pie-noires. Institut Technique de l'Élevage Bovin,  
530 Paris, France.

531 Berman, A., 2003. Effects of body surface area estimates on predicted energy requirements and heat  
532 stress. *Journal of Dairy Science* 86, 3605-3610.

533 Buranakarl, C., Indramangala, J., Koobkaew, K., Sanghuayphrai, N., Sanpote, J., Tanprasert, C.,  
534 Phatrapornnant, T., Sukhumavasi, W., Nampimoon, P., 2012. Estimation of body weight and body  
535 surface area in swamp buffaloes using visual image analysis. *Journal of Buffalo Science*, 1, 13-20.

536 Cignoni, P., Callieri, M., Corsini, M., Dellepiane, M., Ganovelli, F. Ranzuglia, G., 2008. MeshLab: an  
537 Open-Source Mesh Processing Tool. Sixth Eurographics Italian Chapter Conference, 129-136.

538 Elting, E.C., 1926. A formula for estimating surface area of dairy cattle. *Journal of Agriculture*  
539 *Research* 33, 3, 269-279.

540 Fischer, A., Luginbuhl, T., Delattre, L., Delouard, J. M., Faverdin, P., 2015. Rear shape in 3 dimensions  
541 summarized by principal component analysis is a good predictor of body condition score in Holstein  
542 dairy cows. *Journal of Dairy Science* 98, 4465 - 4476.

543 Guo H., Ma, X., Ma, Q., Wang, K., Su, W., Zhu D., 2017. LSSA\_CAU: an interactive 3d point clouds  
544 analysis software for body measurement of livestock with similar forms of cows and pigs.  
545 *Computers and Electronics in Agriculture*, 138, 60-68.

546 Halachmi, I., Polak, P., Roberts, D.J., Klopcic, M., 2008. Cow body shape and automation of condition  
547 scoring. *Journal of Dairy Science*, 91, 4444-4451.

548 Heinrichs, A.J., Rogers, G.W., Cooper, J.B., 1992. Predicting body weight and wither height in Holstein  
549 heifers using body measurements. *Journal of Dairy Science*, 75 (12), 3576-3581.

550 Kazhdan, M., Hoppe, H., 2013. Screened Poisson surface reconstruction. *ACM Transactions on*  
551 *Graphics*, 32 (3), Article 29.

552 Kuzuhara, Y., Kawamura, K., Yoshitoshi, R., Tamaki, T., Sugai, S., Ikegami, M., Kurokawa, Y., Obitsu,  
553 T., Okita, M., Sugino, T., Yasuda, T., 2015. A preliminary study for predicting body weight and milk  
554 properties in lactating Holstein cows using a three-dimensional camera system. *Computers and*  
555 *Electronics in Agriculture*, 111, 186-193.

556 Le Cozler Y, Allain A, Caillot A, Delouard JM, Delattre L, Luginbuhl T, Faverdin P 2019. High precision  
557 scanning system for complete 3D cow body shape imaging and analyzing morphological traits.  
558 *Computers and electronics in Agriculture* 157,447-453.

559 Marchant, J.A., Schofield, C.P., 1993. Extending the snake image processing algorithm for outlining  
560 pigs in scenes. *Computers and Electronics in Agriculture*, 8, 261-275.

561 Minagawa, H., 1994. Surface area, volume, and projected area of Japanese-shorthorn cattle  
562 measured by stereo photogrammetry using non-metric cameras. *Journal of Agriculture Met* 50(1),  
563 17-22.

564 Mirtich, B., 1996. Fast and accurate computation of polyhedral mass properties. *Journal of Graphics*  
565 *Tools* 1 (2), 31-50.

566 Mortensen, A.K., Lisouski, P., Ahrendt, P., 2016. Weight prediction of broiler chickens using 3D  
567 computer vision. *Computers and Electronics in Agriculture*, 123, 319-326.

568 Negretti, P., Bianconi, G., Bartocci, S., Terramoccia, S., Verna, M., 2008. Determination of live weight  
569 and body condition score in lactating Mediterranean buffalo by Visual Image Analysis. *Livestock*  
570 *Science*, 113, 1-7.

571 Pezzuolo, A., Guarino, M., Sartori, L., Marinello, F., 2018. A feasibility study on the use of a structured  
572 light depth-camera for three-dimensional body measurements of dairy cows in free-stall barns.  
573 *Sensors*, 18, 673, doi: 10.3390/s18020673.

574 Pezzuolo, A., Guarino, M., Dartori, L., Gonzalez, L.A., Marinello, F., 2018. On-barn pig weight  
575 estimation based on body measurements by a Kinect v1 depth camera. *Computers and Electronics*  
576 *in Agriculture*, 148, 29-36.

577 R Core Team 2019. R: a language and environment for statistical computing. R Foundation for  
578 Statistical Computing, Vienna, Austria. Version 3.2.4. Retrieved 1 April 2016 from [https:// www .r-  
579 project.org/](https://www.r-project.org/).

580 Schofield C. P., Marchant J. A., White R. P., Brandl N., Wilson M. 1999. Monitoring of pig growth using  
581 prototype imaging system. *Journal of Agricultural Engineering Research*, 72, 3, 205-210.

582 Spoliansky, R., Edan, Y., Parmet, Y., Halachmi, I., 2016. Development of automatic body condition  
583 scoring using a low-cost 3-dimensional Kinect camera. *Journal of Dairy Science*, 99, 9, 7714 -  
584 7723.

585 Van Hertem, T., Viazzi, S., Steensels, M., Maltz, E., Anatler, A., Alchanatis, V., Schlageter-Tello, A.A.,  
586 Lokhorst, K., Romanini, E.C.B., Bahr, C., Berckmans, D., Halachmi, I., 2014. Automatic lameness  
587 detection based on consecutive 3D-video recordings. *Biosystems Engineering*, 119, 108-116.

588 Wang, K., Guo, H., Ma, Q., Su, W., Chen, L., Zhu, D., 2018. A portable and automatic Xtion-based  
589 measurement system for pig body size. *Computers and Electronics in Agriculture*, 148, 291-298.

590 Zhao, K., Bewley, J.M., Heade, D., Jin, X., 2018. Automatic lameness detection in dairy cattle based  
591 on leg swing analysis with an image processing technique. *Computers and Electronics in*  
592 *Agriculture*, 148, 226-236.